



INTERNATIONAL JOURNAL OF CREATIVE RESEARCH THOUGHTS (IJCRT)

An International Open Access, Peer-reviewed, Refereed Journal

ESTIMATION OF NOISE IN HYPER SPECTRAL REMOTE SENSING IMAGES USING CURVELET TRANSFORM

¹Thirumala Lakshmi K, ²Mugambika, ³Saraswathi, ⁴Uchimakali

¹Student, ²Assistant professor, ^{3,4}Student

¹Department of Electronics and Communication Engineering,

¹University V.O.C College of Engineering, Tuticorin, India

Abstract: In this paper, the author have attempted to estimate the noise in hyperspectral images over the belt of 35⁰N to 35⁰S and 118⁰E to 118⁰W from the satellite AVIRIS images obtained from JPL, NASA for the period October 1992. The paper aims in particular, to find out the thresholding technique and image transform for satellite image denoising. For this purpose the authors have investigated a few threshold techniques and wavelet transforms. The study shows that the curvelet transform is better than wavelet transform for noise estimation in hyperspectral images.

Index Terms – Hyper spectral image, denoise, wavelet transform, curvelet transform, threshold

I. INTRODUCTION

Hyperspectral remote sensing images (HRSI) are often viewed as three-dimensional data consisting of one-dimensional spectral information and two-dimensional spatial information (Geo University, 2020). Multi-spectral remote sensors namely Landsat Thematic Mapper, and SPOT XS produce images with a few relatively broad wavelength bands (Sciencedirect, 2019). Hyperspectral remote sensors collect image data simultaneously in dozens or hundreds of narrow, adjacent spectral bands. With the fast development of hyperspectral remote sensing technology, HRSI can extract the feature and attributes of Earth objects more accurately and therefore, it's broadly applied in many fields namely agriculture, forestry, environmental monitoring, weather study, military recon, etc. Although over the last decades the event of imaging spectrometers is rapid, HRSI remains suffering from many complex factors during the processing of acquisition and transmission, which can produce more noise. The reliability of the information delivered by hyperspectral remote sensing applications highly depends on the quality of the captured data. The noise includes a signal-dependent (SD) component, called photon noise, and signal-independent (SI) components, called dark noise (Acito et al, 2011, Peng Fu et al, 2018). The signal-dependent noises are noises that vary according to the variation of signal amplitude, frequency, etc and the signal independent noises are due to the nonlinear nature of scattering. Due to the presence of noise in the image, the research leads to failure to extract the valuable information and further research interpretation. The presence of noise in HRSI affects to detect the target of image classification, and segmentation, so it's vital to study about the characteristic of HRSI for denoising.

When the sunlight propagates through the atmosphere to reach Earth, the atmosphere layer often reflects, refracts, and scatters light; thus the electromagnetic waves propagation path of hyperspectral imaging will also get affected by many complex factors that introduce noise. The noise type and parameters are quite important for its post-processing and application, so it is very necessary to study the noise estimation of hyperspectral remote sensing images. Comparing with a normal three-dimensional data cube of the fixed variance of additive noise, the noise level of the hyperspectral image may vary dramatically from band to band. The standard deviation and variance of hyperspectral image vary from band to band. That is, the level of the noise is dependent on the average amplitude of each band but spatially stationary in each band.

Anish Mohan et al. (2013) proposed a non-linear dimensionality reduction and vector segmentation of hyperspectral images is investigated for the classification and clustering of hyper-spectral data. Hyperspectral sensors such as AVIRIS deliver calibrated images of 224 contiguous spectral channels (bands), with wavelengths from 400 to 2500 nm is a data cube. The amount of data that is acquired may typically run into hundreds of megabytes. The main problem is reducing the huge amount of data into tractable levels. The redundancy in the data of adjacent bands is intrinsically exploited to help in this data reduction. Simultaneously this data reduction also removes spurious and erroneous information from the data, thereby leading to more accurate clustering and classification. Most of the methods do not consider the nonlinear characteristics of the hyper-spectral data. This method effectively reduced the amount of noise with 75% accuracy. Dong Xu et al. (2013) proposed a new denoising algorithm of hyperspectral remote sensing image (HRSI) in the curvelet domain to denoise both signal-dependent noises and signal independent noise. Shen-En and Chen (2007) combine Locally Linear Embedding (LLE) with Laplacian Eigenmaps for hyper-spectral data. Othman and Qian (2006) worked with AVIRIS image for vegetation dominated site and geo location site. Atkinson et al. (2003) proposed a novel DFT and WT to estimate SNR and the research obtained gain of 14 dB.

Wavelet is a good time-frequency localization and multi-resolution analysis property; it is successfully and widely applied in several fields. It is not perfect representation tool to extract features for anisotropic singularities, but it is good tool for isotropic singularity i.e it is weak for curves but good for point singularity. To overcome the drawbacks of wavelet transform, the complex wavelet transform, curvelet transform, and contourlet transform are proposed. The curvelet decomposition follows subband decomposition, smooth partitioning, renormalization, and ridgelet transform. The major drawback of wavelet transform is that it cannot represent 2-D image with edge sparsely and also it capture information in the direction of vertical, horizontal and diagonal directions. However, the curvelet obtain detailed preservation of the image and remove the noise in HRSI more accurately than wavelet transform.

II. DATA AND METHODOLOGY

The authors made an attempt to estimate the noise from hyperspectral satellite images for the period October 1992. The noise estimation is carried out on AVIRIS image provided by JPL, NASA. The scene request ID is f921014t0p02-r05. The study covers the belt of 35°N to 35°S and 118°E to 118°W. The size of the data cube for an image is 312*312*40. The parameter measured for image quality is signal to noise ratio (SNR). The collected HRSI images are given to two transforms namely wavelet transform and curvelet transform. The parameter SNR is estimated using these two transforms. Then both transforms results are compared to check the accuracy of image denoising. Figure 1 shows the work flow to estimate noise.

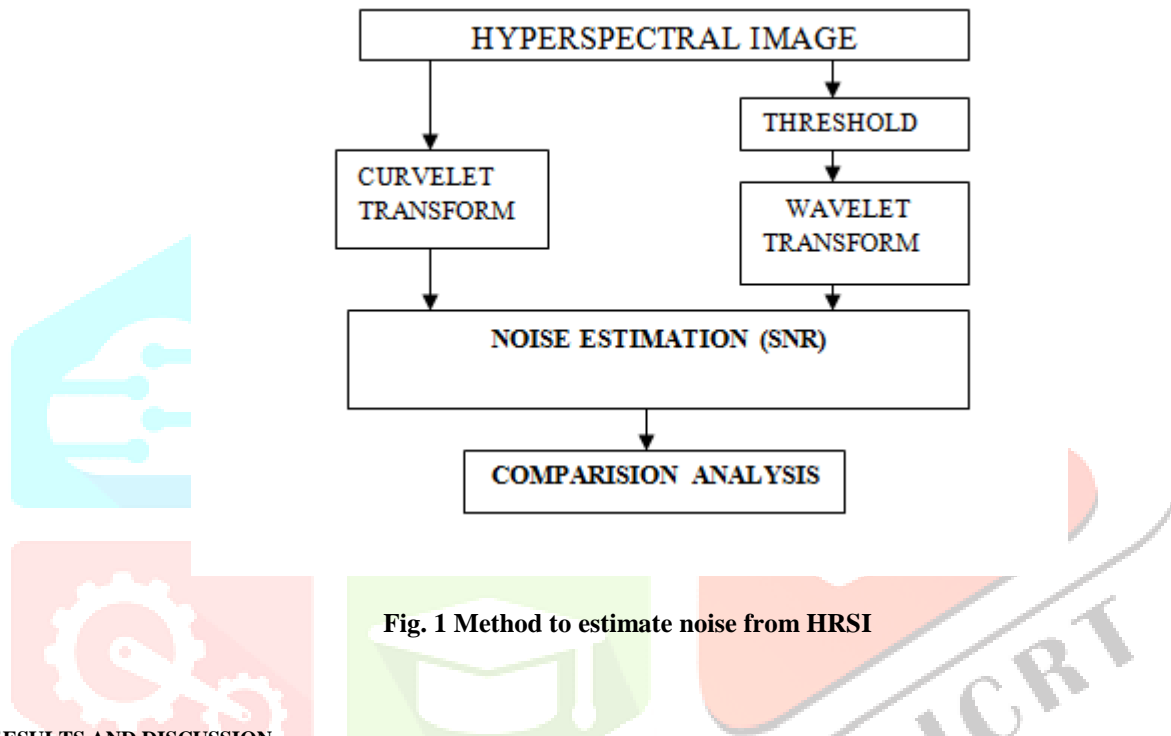


Fig. 1 Method to estimate noise from HRSI

III. RESULTS AND DISCUSSION

To get rid of the spatial correlation of a hyperspectral image, the wavelet transform is employed, then the extent of the noise are often better estimated. Wavelet transform, transforms the image into a replacement presentation domain by multi-scale transform and decouples the higher-order statistical characteristic of natural images, therefore the signal power is concentrated within the low-frequency sub bands of the wavelet coefficients, on the contrary, the high-frequency sub bands of the wavelet coefficients describe the signals which change sharply or are discontinuous. Since the wavelet transform is orthogonal, Gaussian noise is scattered throughout the wavelet coefficients domain after the orthogonal transformation and obeys a normal distribution within the new representation domain

Wavelets are powerful tools for image processing, signal processing and data compression. Wavelet transforms are a superb alternative to Fourier transforms in many situations. In Fourier analysis, a sign is decomposed into periodic components; in wavelet analysis, a sign is decomposed into components localized in both time and frequency domains (Thirumala Lakshmi and Usha K D, 2016). Thus, wavelet transforms are ideal when signals aren't periodic. The essential idea behind wavelet transform is to analyze different frequencies of a sign using different scales. To be more specific, in wavelet transform, all of the idea functions, which are called wavelets, are derived from scaling and translation of one function, called mother wavelet. The Daubechies wavelet transform allows an input image to be decomposed into a group of independent coefficients, like each orthogonal basis (Thirumala Lakshmi et al, 2019). Figure 2 shows the wavelet transform of the image.

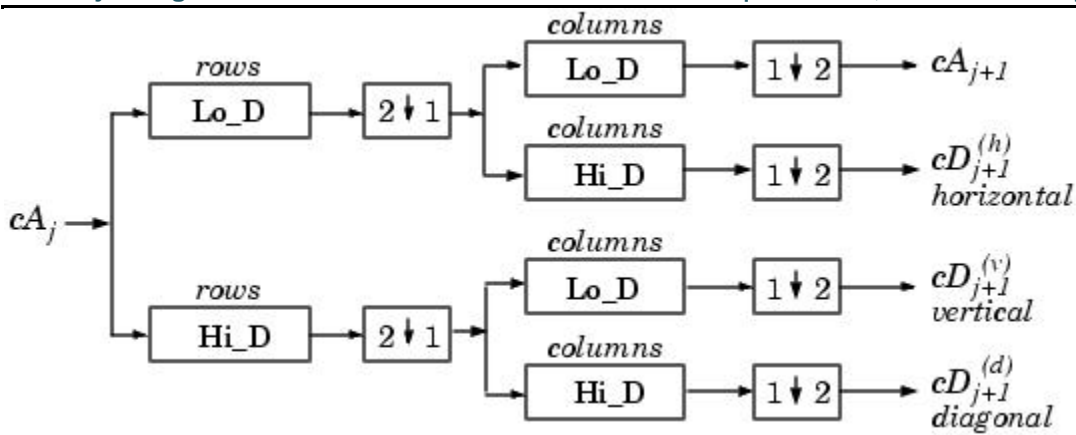


Fig. 2 Flow of wavelet transforms

First, the one-dimensional wavelet transform is applied to each row of the image and then the same transform is applied to each column. Then, the two-dimensional wavelet transform can be implemented by applying the one-dimensional splitting algorithm to the horizontal and vertical lines (namely, rows and columns) of an image, successively. The first sub-image $j+1$ cA is obtained by applying the horizontal low-pass filter and the vertical low-pass filter successively. The second sub-image hj $cD+1$ is obtained by applying the horizontal low-pass filter followed by the vertical high-pass filter. The third sub-image vj $cD+1$ is obtained by applying the horizontal high-pass filter followed by the vertical low-pass filter. Finally, the fourth sub-image dj $cD+1$ is obtained by applying the horizontal and vertical high-pass filters successively. Where $j+1$ cA is the approximation coefficients of an image, hj $cD+1$ is the horizontal coefficients of an image, vj $cD+1$ is the vertical coefficients of an image, and dj $cD+1$ is the diagonal coefficients of an image.

De-noising plays a vital role in the field of image processing. It is often necessary to be taken before the image data is analyzed. It attempts to get rid of whatever noise is present and retains the many information, no matter the frequency contents of the signal. De-noising has got to be performed to recover the useful information. In this step, the edges of the image are preserved well and, the noise granularity in the image has been removed.

The main aim of the image-denoising algorithm is to reduce the noise level while preserving the image features. In the wavelet domain, the noise is uniformly spread throughout the coefficients, while most of the image information is concentrated within the few largest coefficients. Distinguishing the noise from the image has been done by thresholding the wavelet coefficients.

During thresholding, a wavelet coefficient is compared with a given threshold and is about to zero if its magnitude is a smaller amount than the threshold; otherwise, it's retained or modified depending on the threshold rule. The choice of a threshold is a crucial point of interest (Sankar Padmanaban, 2014). It plays a serious role within the removal of noise in images because denoising most often produces smoothed images, reducing the sharpness of the image. There exist various methods for wavelet thresholding, which believe the selection of a threshold value. Some of the methods used for image noise removal are VisuShrink, SureShrink, and BayesShrink. Before to discuss the threshold methods, it is necessary to know about the two general categories of thresholding: hard and soft-threshold. Donoho (1995) proposed both soft and hard threshold technique for images denoise.

Hard threshold may seem to be natural. Noise coefficients may pass the hard threshold and generate annoying output. Thus, all coefficients whose magnitude is greater than the selected threshold value remain as they are and the others with magnitudes smaller than t are set to zero. It creates a region around zero where the coefficients are considered negligible.

Soft threshold shrinks the coefficients above the threshold value. Soft threshold shrink the coefficients towards zero after comparing the coefficients to a threshold value. In practice, it can be seen that the soft method is much better and yields more visually pleasing images, because of the discontinuity and abrupt artifacts in the recovered images (Soft threshold, 2020). Also, the soft method yields a smaller minimum mean squared error compared to the hard form of thresholding. Nowadays, wavelet-based denoising methods have received greater attention. In soft threshold, the image is first subjected to a discrete wavelet transform, which decomposes the image into various sub-bands. Figure 3 shows the sub band decomposition.

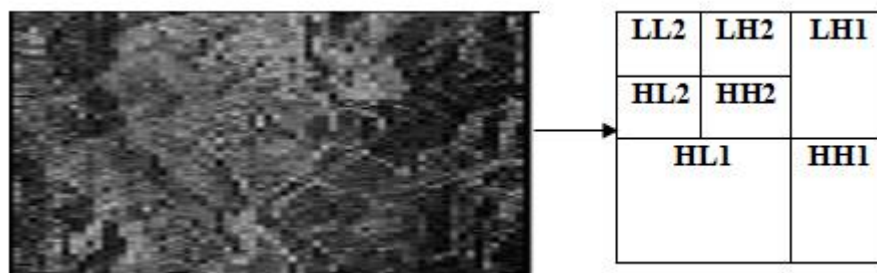


Fig. 3 Sub band Decomposition

The sub-bands HHk , HLk , LHk , $k = 1, 2, \dots, j$ is called the details, where k is the scale and j denotes the largest or coarsest scale in decomposition. LLk is the low-resolution component. Thresholding is now applied to the detail components of these sub-bands to remove the unwanted coefficients, which contribute to noise. And as a final step in the denoising algorithm, the inverse discrete wavelet transform is applied to build back the modified image from its coefficients.

In wavelet decomposition, different wavelet families are used to estimating the noise. The wavelet families utilized in thresholding techniques are Daubechies, coiflet, and haar wavelet transform. Haar wavelet is that the simplest of the wavelet

transforms. Daubechies wavelets which are a family for orthogonal wavelets defining a discrete wavelet transform (Thirumala Lakshmi et al, 2019). Coiflets are discrete wavelets designed by Ingrid Daubechies, to possess scaling functions with vanishing moments (Wikipedia, 2020). By using these transforms the SNR value are calculated. Two shrinkage methods are used up here to estimate the noise in HSI. Shrinkage may be a documented and appealing denoising technique. The most three existing soft thresholding techniques are VisuShrink, Bayes shrink, and Sure shrink (Shivani M et al, 2013).

VisuShrink (Prashant, 2013) is thresholding by applying the universal threshold proposed by Donoho and Johnstone. It uses a threshold value that is proportional to the standard deviation of the noise. It is also referred to as universal threshold and is defined as

$$t = \sigma\sqrt{2\log n} \quad (1)$$

σ is the noise variance present in the signal and n represents the signal size or number of samples. An estimate of the noise level σ was defined based on the median absolute deviation given by

$$\sigma = \text{median} (\{|g_j - 1|; k = 0, 1, \dots, 2^{j-1} - 1\}) / 0.6745 \quad (2)$$

Where $g_j - 1, k$ corresponds to the detail coefficients in the wavelet transform.

For denoising images, visushrink is found to yield an excessively smoothed estimate. It is because of Universal threshold (UT), derived under the constraint that with high probability, The estimate should be at least as smooth as the signal. So Universal threshold (UT) tends to be high for large values of M , killing many signal coefficients along with the noise. VisuShrink does not deal with minimizing the mean squared error. It is often viewed as general-purpose threshold selectors that exhibit near-optimal minimax error properties and ensures with high probability that the estimates are smooth because of the true underlying functions. VisuShrink is known to yield recovered images that are overly smoothed. This is because VisuShrink removes too many coefficients. The disadvantage is that it cannot remove speckle noise. It can only deal with additive noise. VisuShrink follows the worldwide thresholding scheme where there's one value of threshold applied globally to all or any of the wavelet coefficients.

A threshold chooser supported Stein's Unbiased Risk Estimator (SURE) was proposed by Donoho and Johnstone and is named as SureShrink (Shivani M et al, 2013). It's a mixture of the universal threshold and therefore the SURE threshold. This method specifies a threshold value t_j for every resolution level j within the wavelet transform which is mentioned as level dependent thresholding. The goal of SureShrink is to minimize the mean squared error, defined as

$$MSE = \frac{1}{n^2} \sum_{x,y=1}^n (z(x,y) - s(x,y))^2 \quad (3)$$

where $z(x,y)$ is the estimate of the signal while $s(x,y)$ is the original signal without noise and n is the size of the signal. SureShrink suppresses noise by thresholding the empirical wavelet coefficients. The SureShrink threshold t^* is defined as

$$t = \min(t, \sigma\sqrt{2\log n}) \quad (4)$$

where t denotes the value that minimizes Stein's Unbiased Risk Estimator, σ is the noise variance computed and n is the size of the image. SureShrink follows the soft thresholding rule. The thresholding employed here is adaptive, a intensity is assigned to every dyadic resolution level by the principle of minimizing Stein's Unbiased Risk Estimator for threshold estimates. It's smoothness adaptive, which suggests that if the unknown function contains abrupt changes or boundaries within the image, the reconstructed image also does. BayesShrink was proposed by Chang, Yu, and Vetterli (Khlifa et al, 2009). The goal of this method is to attenuate the Bayesian risk, and hence its name, BayesShrink. It uses soft thresholding and is subband-dependent, which suggests that thresholding is completed at each band of resolution within the wavelet decomposition. Bayes shrink is image denoising adaptive data-driven soft thresholding. The edge is driven within the Bayesian framework and it assumes Generalized normal distribution (GGD) for the wavelet coefficient in each detail sub-band and tries to seek out the edge T minimizes the Bayesian Risk. Just like the SureShrink procedure, it is smoothness adaptive. The Bayes threshold, t_B , is defined as

$$t_B = \sigma^2 / \sigma_s \quad (5)$$

Where σ^2 is the noise variance and σ_s is the signal variance without noise. The noise variance σ^2 is estimated from the subband HH1 by the median estimator. From the definition of additive noise we have

$$w(x,y) = s(x,y) + n(x,y) \quad (6)$$

Since the noise and the signal are independent of each other, it can be stated that

$$\sigma^2 w = \sigma^2 s + \sigma^2 \quad (7)$$

$\sigma^2 w$ can be computed as shown below:

$$\sigma^2 w = 1/n^2 \sum_{x,y=1}^n w^2(x,y) \quad (8)$$

The variance of the signal, $\sigma^2 s$ is computed as

$$\sigma^2 s = \sqrt{\max(\sigma^2 w - \sigma^2)} \quad (9)$$

With $\sigma^2 s$ and σ^2 is the Bayes threshold. Using this threshold, the wavelet coefficients are thresholded at each band. The BayesShrink performs better than sure shrink in terms of MSE and therefore the sharp features of the image are retained. But MSE is considerably lower. This is often because sure shrink is subband adaptive. On comparing this threshold method, Bayes shrink is best. The SNR values are far better than visushrink and therefore the threshold value obtained by the Bayes shrink method is extremely high in comparison to the opposite method. Since wavelet has good time-frequency-localization property and multiresolution analysis property, it's widely and successfully applied in several fields. However, the wavelet isn't perfect. Wavelet is especially applied to the representation of isotropic singularity object, while for anisotropic singularities, like boundary and linear features of a picture, it's not an honest representation tool. In other words, wavelet may be a good representation for point singularity, except for the curves, it's relatively weak. Hence to beat this drawback the curvelet transform is employed. In Fourier transform a discontinuity point affects all the Fourier coefficients within the domain. Point discontinuities are not handled by Fourier. In wavelet transform some extent affects only a limited number of coefficients. Discontinuities across the straightforward curve affect all the wavelet coefficients within the curve. WT handles point discontinuities not curve discontinuities well. But a curvelet is meant to handle curves using only a little number of coefficients. Hence curvelet transform handles curve discontinuities well. Figure 4 (a-e) shows the output of coif1 WT, coif2 WT, haar WT, db2 WT, and db4 WT, respectively.

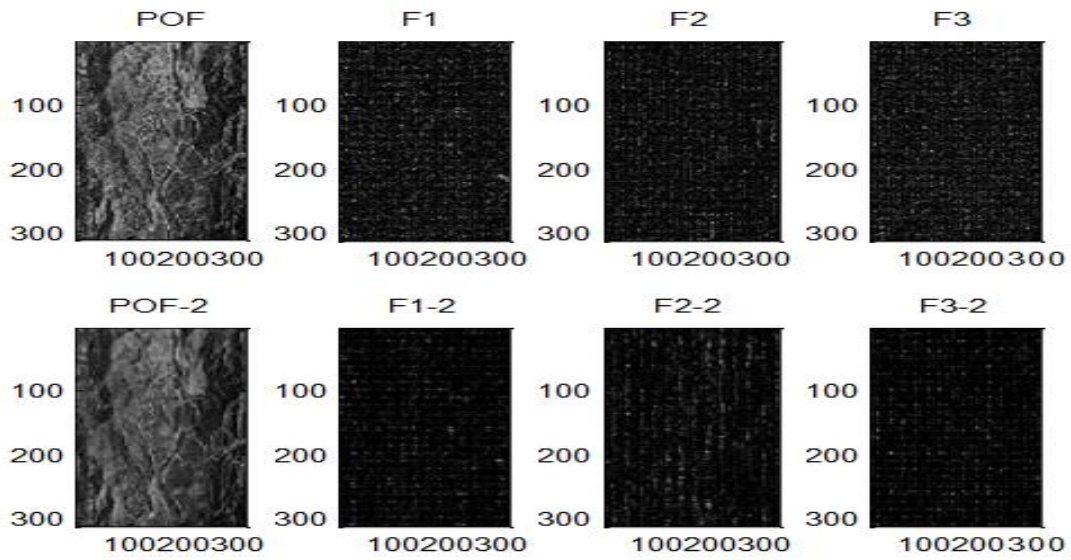


Fig. 4a Output for coif1 WT

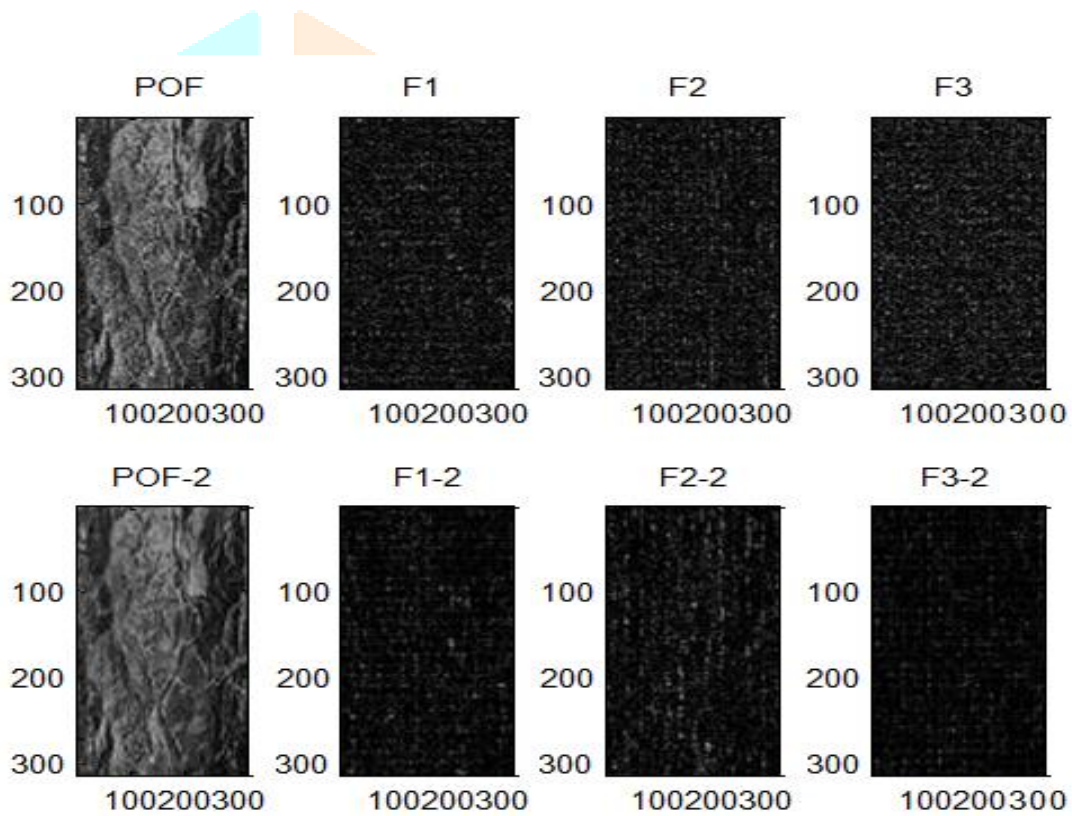


Fig. 4b Output for coif2 WT

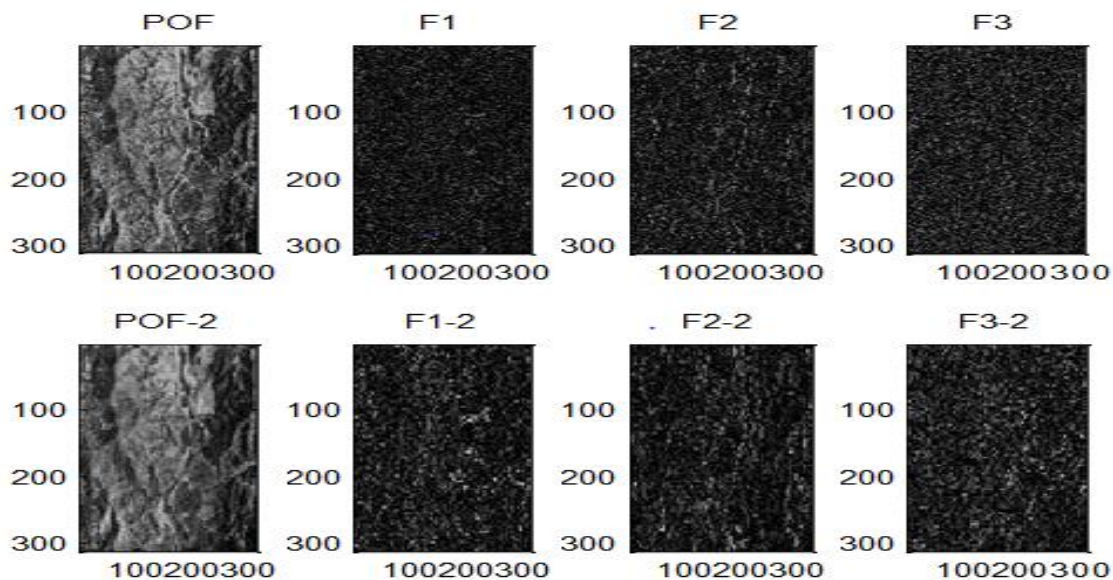


Fig. 4c Output for Haar WT

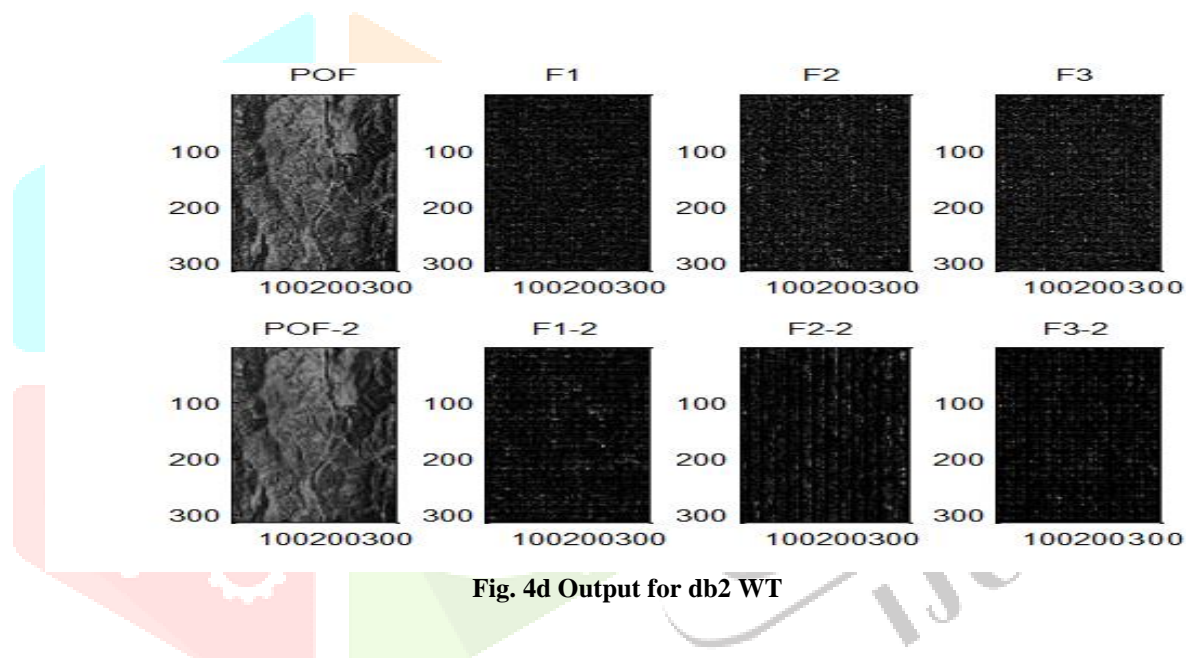


Fig. 4d Output for db2 WT

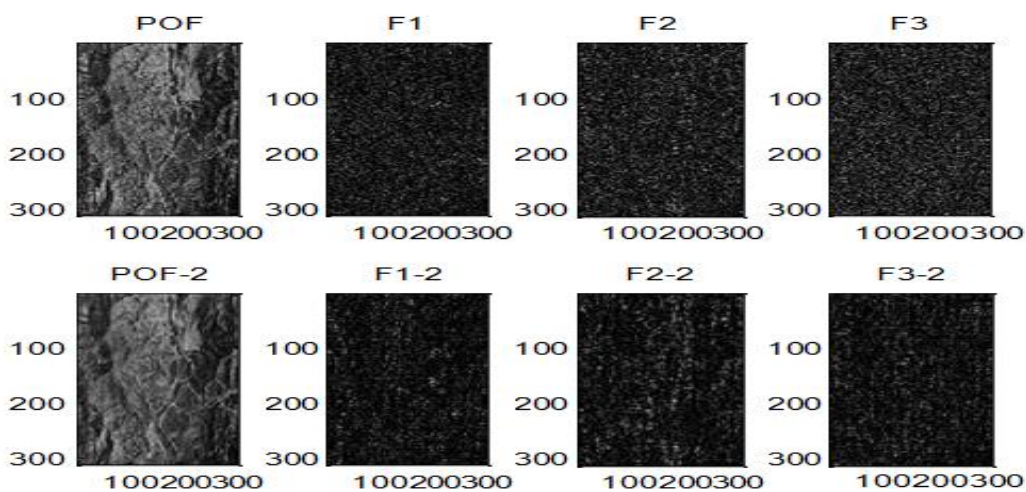


Fig. 4e Output for db4 WT

The input hyperspectral image is divided into different resolution layers by using wavelet transforms. Each layer contains the details of different frequencies. The two-level wavelet decomposition is taken to estimate noise in the image. The wavelet families used here are Daubechies, coiflet, and haar wavelet transform. Figure 5 shows the output of soft threshold image.

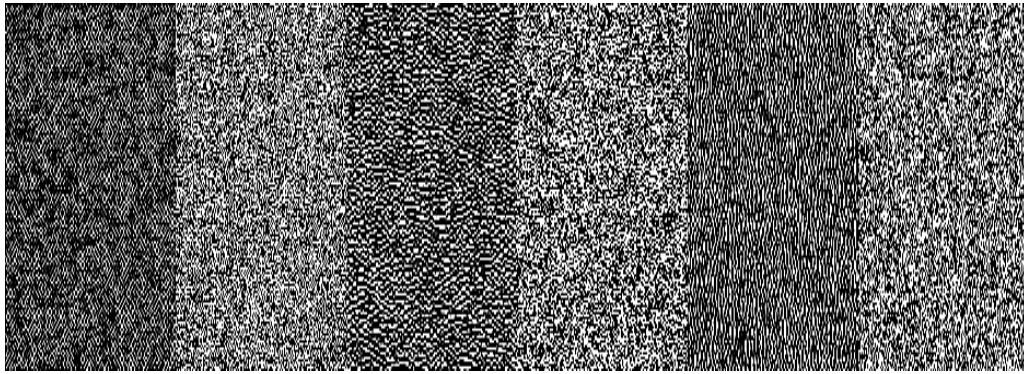


Fig. 5 Output for thresholded image

Table 1 shows the SNR value for first 4 bands (B1-B4). The threshold value for Haar and Db1 is 0.524. The Db2, Db5 and Coif1 WT is 0.5020, and the threshold value is 0.4980 for Db3, Db4, Db6- Db8, and Coif2-Coif3. The noise in B4 band is higher than B1-B3 bands in all transforms. The Db5 estimates low noise in B3 band.

Table 1 SNR value using soft threshold

WAVELET FAMILY	THRESHOLD VALUE	SNR VALUE			
		B1	B2	B3	B4
Haar	0.5294	9.1863	10.529	11.221	7.4002
Db1	0.5294	10.379	9.6680	9.1863	7.4002
Db2	0.5020	9.3824	11.393	9.0132	6.7576
Db3	0.4980	9.0568	11.296	10.034	6.7352
Db4	0.4980	8.8761	9.0804	9.4190	6.7241
Db5	0.5020	10.989	8.2806	11.434	6.7233
Db6	0.4980	8.3357	9.0390	9.0591	6.735
Db7	0.4980	11.332	10.714	9.0979	6.7241
Db8	0.4980	8.7098	11.351	10.054	6.7241
Coif1	0.5020	9.1148	11.113	9.3998	6.7686
Coif2	0.4980	9.1114	9.0309	6.6901	6.7352
Coif3	0.4980	9.1171	8.4555	9.0530	6.7241

Table 2 shows the SNR value of Bayes shrink and Visu shrink. From Table 1 and 2, it shows that the Db1, Db5-Db8, Coif2-Coif3 and Haar WT estimate noise better in Bayes shrink than Sure shrink and Visu shrink. The accuracy of Bayes shrink is 83.29 %.

Table 2 SNR value Comparison for Bayes and Visu shrink method

WAVELET TRANSFORM	SNR VALUE (BAYES SHRINK)				SNR VALUE (VISU SHRINK)			
	B1	B2	B3	B3	B1	B2	B3	B3
Db1	15.02	15.08	14.88	16.43	13.23	13.21	13.25	10.12
Db2	14.91	14.89	15.03	23.09	16.06	15.69	15.46	9.176
Db3	15.14	14.79	14.85	24.90	15.21	15.27	15.56	9.199
Db4	15.36	15.72	15.36	19.83	15.41	15.05	15.20	10.01
Db5	15.40	15.88	15.58	21.01	14.69	14.86	14.69	11.19
Db6	15.96	15.58	15.70	21.23	14.40	14.78	14.18	11.61
Db7	15.75	15.66	15.84	19.04	14.71	14.57	14.81	11.31
Db8	15.29	15.24	15.28	20.99	14.70	14.90	14.76	10.17
Coif1	15.87	15.97	16.09	20.85	16.64	16.56	16.67	11.62
Coif2	16.16	16.05	16.66	20.02	14.87	15.32	14.90	11.60
Coif3	16.50	16.32	16.39	20.84	14.75	14.73	15.10	11.61
Haar	14.98	15.19	15.01	16.28	13.22	13.23	13.24	10.12

The ridgelet transform is that the core spirit of the curvelet transforms (Starck et al, 2002). The ridgelet transform is perfect at representing straight-line singularities. Unfortunately, global straight-line singularities are rarely observed in real applications other than ridgelet transform to obtain sub-images. This block ridgelet-based transform is known as curvelet transform. which is called first-generation curvelet transform because the geometry of ridgelets is unclear, as they're not true ridge functions in images. The second-generation curvelet transform may be a very efficient tool for several different applications in image processing. The curvelet transform may be a multiscale directional transform that permits an almost optimal non-adaptive sparse

representation of the thing with edges. The curvelet transform is often decomposed into four-step: Subband Decomposition, Smooth Partitioning, Renormalization, and Ridgelet Analysis. By inverting the step sequence with mathematic revising, it can reconstruct the first signal which is named inverse curvelet transform. Ridgelet transform details the 2D image with a line. But in most images there are many curves, so we must divide the image into pieces. To urge a far better result the image is decomposed into a sub-band, and divide these images with different scales into pieces. This type of multi-level and multi-scale ridgelet transform is named curvelet transform. Figure 6 shows the flow of curvelet transform.

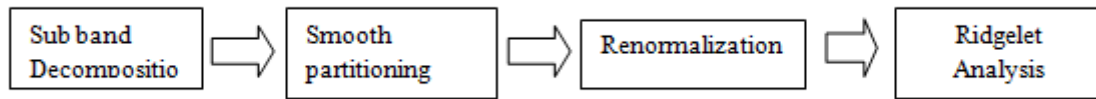


Fig. 6 Flow of curvelet transforms

To finish the ridgelet transform, a 1-D wavelet transform is taken along the radial variable in Radon space. Due to the shortage of localization of compactly supported wavelets within the frequency domain, fluctuations in coarse-scale wavelet coefficients can introduce fine-scale fluctuations; but this is often undesirable so here the frequency-domain approach, where the discrete Fourier transform is reconstructed from the inverse Radon transform. The wavelet transform algorithm is predicated on a scaling function that vanishes outside of the interval. The wavelet transform has the subsequent features. The wavelet coefficients are directly calculated within the Fourier space. Within the context of the ridgelet transform, this enables avoiding the computation of the 1-D inverse Fourier transform along each radial line. Subband is sampled above the Nyquist rate, to avoid aliasing and this phenomenon encountered by sampled orthogonal wavelet transforms. The reconstruction is trivial. The wavelet coefficients simply got to be co-added to reconstruct the input at any given point. In our application, this suggests that the ridgelet coefficients simply got to be co-added to reconstruct Fourier coefficients. This wavelet transform introduces an additional redundancy factor, which could be viewed as an objection by advocates of orthogonality and importance sampling. The ridgelet transform of a picture of size $n \times n$ is a picture of size $2n \times 2n$, introducing a redundancy factor adequate to four.

Although the wavelet transforms established a powerful reputation as a tool for signal processing, it's the disadvantage of poor directionality, which has undermined its usage in many applications. Significant progress within the development of directional wavelet has been made in recent years. Within the necessity of anisotropic transform, a multiresolution geometric analysis, named curvelet transform was proposed. Being the extension of wavelet, it did make a powerful performance in image denoising and therefore the result shows that it performs far better in image denoising. Figure 7 shows the subband decomposition of curvelet transform.

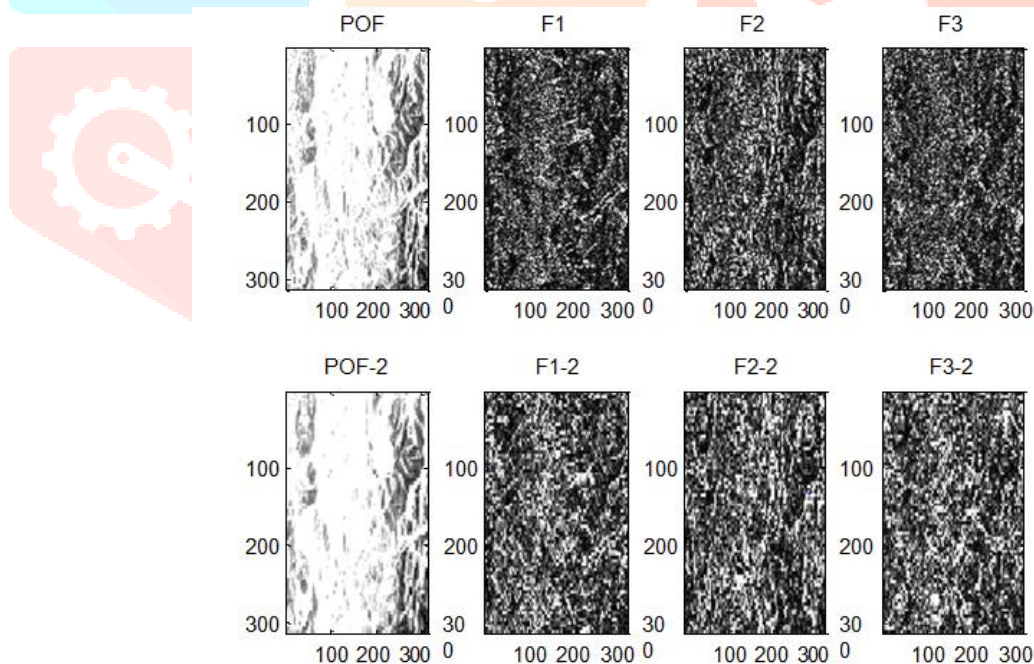


Fig. 7 sub-band decomposition output

The input hyperspectral image is divided into different resolution layers. Each layer contains the details of different frequencies. Where pof, pof-1 denotes low pass filters and f1, f2, f3, ..., are high pass filters that are bandpass filters. The original image can be reconstructed from the subbands. Then each sub-band image is divided using a dyadic square of size $2^{-s} \times 2^{-s}$ and then these sub-band images get smoothed by using the smooth windowing function W . Figures 8-10 show the block partition, smooth partition and renormalization output, respectively. The image becomes smooth after multiplying w_0 function. The partitioning makes us easier to analyze local line or curve singularities. Each bands in the images get renormalized to unit square $[0,1] \times [0,1]$.

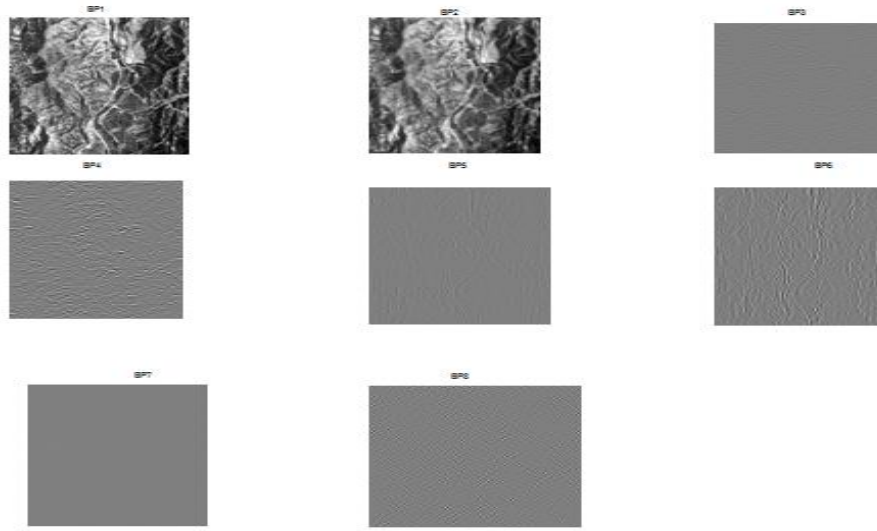


Fig. 8 Block partitioning output

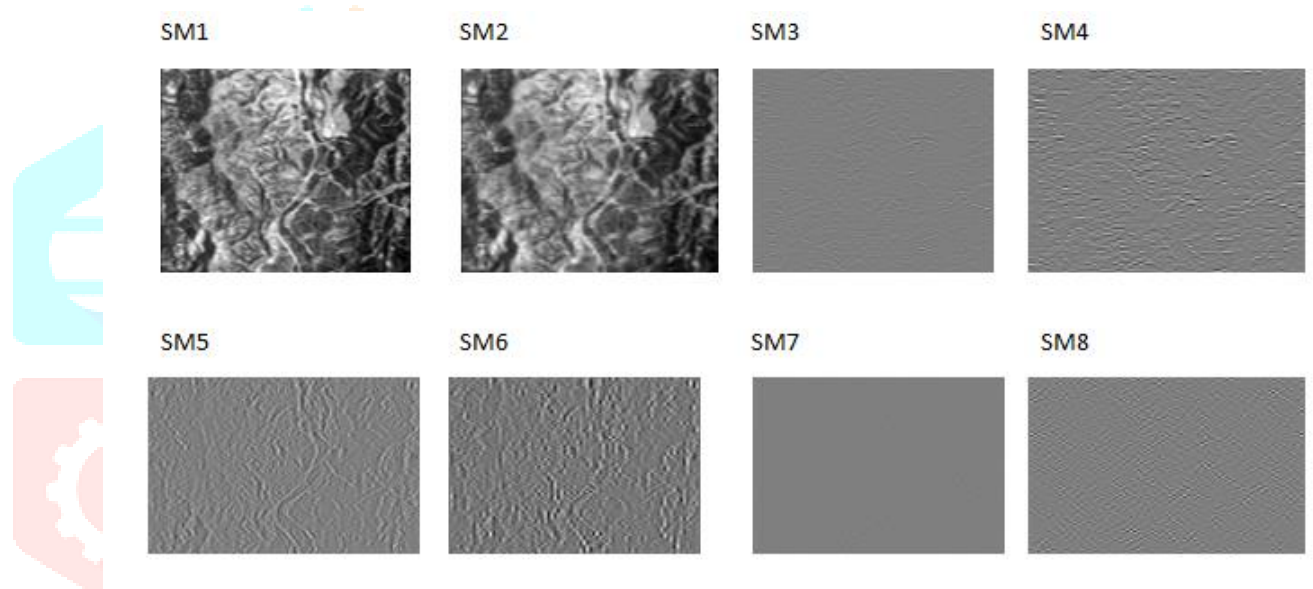


Fig. 9 Smooth partitioning output

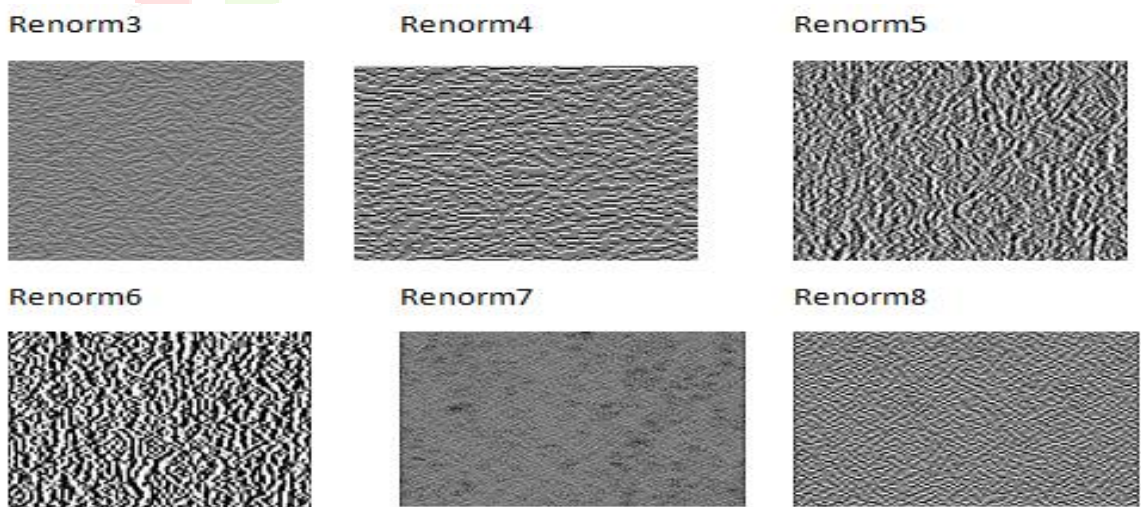


Fig. 10 Renormalization output

Table 3 shows the SNR value of curvelet transform. It is known that the SNR value obtained by the Curvelet transform is better than the SNR value obtained by the Wavelet transform. So for image denoising curvelet transform is best than wavelet transform. Figure 11 shows the accuracy of wavelet and curvelet transform for image denoising in HRSI. From figure 11, it shows that the accuracy of curvelet transform is higher than wavelet transform.

Table 3 Curvelet transform output

Curvelet Transform	SNR VALUE			
	B1	B2	B3	B4
Db1	24.75	24.76	24.75	24.94
Db2	23.35	23.33	23.38	24.10
Db3	23.78	23.79	23.71	24.56
Db4	24.02	24.02	23.97	24.10
Db5	24.06	24.10	24.09	24.30
Db6	24.03	24.03	24.09	24.46
Db7	24.10	24.11	24.15	24.75
Db8	24.30	24.21	24.39	24.99
Coif1	24.55	24.58	24.59	24.90
Coif2	24.50	24.46	24.50	24.93
Coif3	24.49	24.45	24.51	24.97
Haar	24.78	24.74	24.76	24.94

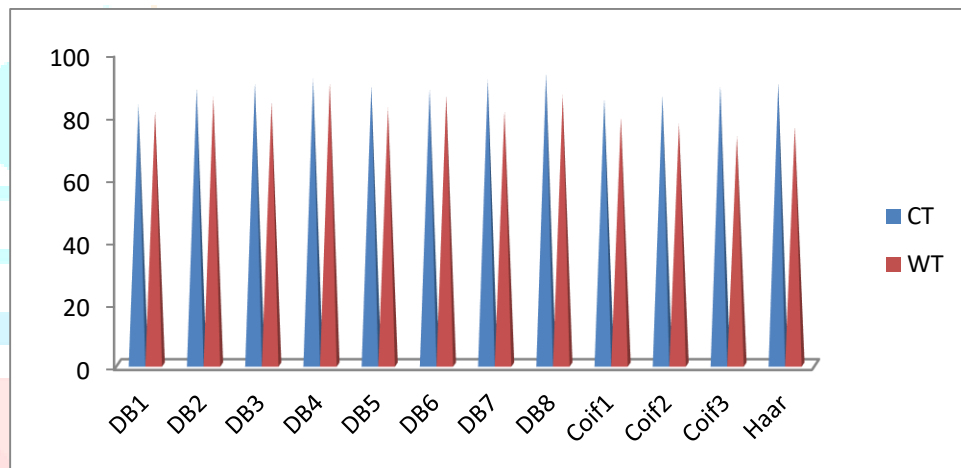


Fig. 11 Accuracy of curvelet and wavelet transform

IV. CONCLUSION

Estimate noise in hyperspectral remote sensing images is vital and more necessary for many applications. To estimate the noise within the Hyperspectral image both wavelet and curvelet transform are used. In wavelet transform, the wavelet thresholding method is employed to estimate the noise within the image. The thresholding methods are VisuShrink, SureShrink, and BayesShrink. Among these, Bayes Shrink gave the best results. Then the curvelet transform is employed. The curvelet transform is followed by sub-band decomposition and ridgelet analysis. A crucial parameter to calculate the image quality is signal to noise ratio. On comparing both these transforms Curvelet transform is best. The SNR value obtained for curvelet transform is better than wavelet transform. Hence the curvelet transform is that the effective method for image denoising than wavelet transform.

V. ACKNOWLEDGMENT

I would like to acknowledge JPL, NASA for providing the satellite images. I feel elated in manifesting a sense of gratitude and thankfulness to my co authors.

REFERENCES

- [1] <https://www.geo.university/pages/hyperspectral-remote-sensing>, 2020
- [2] <https://www.sciencedirect.com/topics/earth-planetary-sciences/multispectral-scanner>, 2019
- [3] Acito, N., Diani, M. and Corsini, G. 2011. Signal-Dependent Noise Modeling and Model Parameter Estimation in Hyperspectral Images. *IEEE Transactions on Geoscience and Remote Sensing*, 49(8).
- [4] Peng Fu, Xin Sun. and Quansen. 2018. Estimation of signal-dependent and independent noise from hyperspectral images using wavelet-based superpixel model. *Remote Sensing Letters*, 9(9).
- [5] Anish Mohan, Guillermo Sapiro. and Edward Bosch. 2009. Spatially-Coherent Non-Linear Dimensionality Reduction and Segmentation of Hyper-Spectral Images. Institute for Mathematics and its Applications, University of Minnesota.
- [6] Dong Xu, Lei Sun. and Jianshu Luo. 2013. Denoising of hyperspectral remote sensing image using multiple linear regression and wavelet shrinkage. *Proceedings of International Conference on Information, Business and Education Technology*.
- [7] Shen-En Qian. and Guangyi Chen. 2007. A New Nonlinear Dimensionality Reduction Method with Application to Hyperspectral Image. *IEEE International Geoscience and Remote Sensing*. 2.
- [8] Othman H. and S. E. Qian. 2006. Noise reduction of hyperspectral imagery using hybrid spatial-spectral derivative-domain wavelet shrinkage. *IEEE Transactions on Geoscience and Remote Sensing*. 44(2).
- [9] Atkinson, I, Kamalabadi, F. and Jones, D. L. 2003. Wavelet-based hyperspectral image estimation. *IEEE International Geoscience and Remote Sensing Symposium*.
- [10] Thirumala Lakshmi K. and Usha K D. 2016. Hierarchical semantic classification. *International Journal of Engineering Research Online*, 4(6).
- [11] Thirumala Lakshmi K, Mugambika. And Thayammal. 2019. Classification of Mammogram images. *International Journal of Recent Advances in Signal & Image Processing*, 3(1).
- [12] Sankar Padmanaban. 2014. Denoising of ECG signals using the framelet transform. *International Journal of Computer Applications*, 7(7).
- [13] Donoho, L. 1995. De-noising by soft-thresholding. *IEEE Transactions on Information Theory*, 41(3).
- [14] <https://svi.nl/SoftThreshold>, 2020
- [15] <https://en.m.wikipedia.org/wiki/Coiflet>, 2020
- [16] Shivani, M. and Naga Venkata B. 2013. Comparison of various threshold techniques of image denoising. *International Journal of Engineering Research and Technology*, 2(9).
- [17] Prasanth. L. Parmar. 2013. Image denoising using vushushrink algorithm. *Journal of Information Knowledge and Research in Electronics and Communication Engineering*, 2(2).
- [18] Khelifa, N, Gribaa, N, Mbazaa, I. and Kamal H. 2009. A based Bayesian wavelet thresholding method to enhance nuclear image. *International Journal of Biomedical Imaging*.
- [19] Starck, J L, Candes, E J. and Donoho, D L. 2002. The curvelet transform iage denoising. *IEEE*, 11(6).

